Molecular Cancer Therapeutics

Targeting c-MYC in Platinum-Resistant Ovarian Cancer

Jeyshka M. Reyes-González[1], Guillermo N. Armaiz-Peña[2], Lingegowda S. Mangala[3], Fatma Valiyeva[4], Cristina Ivan[3], Sunila Pradeep[2], Ileabett M. Echevarría-Vargas[1], Adrian Rivera-Reyes[5], Anil K. Sood[2,3,6], and Pablo E. Vivas-Mejía[1,4]

Abstract

The purpose of this study was to investigate the molecular and therapeutic effects of siRNA-mediated c-MYC silencing in cisplatin-resistant ovarian cancer. Statistical analysis of patient's data extracted from The Cancer Genome Atlas (TCGA) portal showed that the disease-free (DFS) and the overall (OS) survival were decreased in ovarian cancer patients with high c-MYC mRNA levels. Furthermore, analysis of a panel of ovarian cancer cell lines showed that c-MYC protein levels were higher in cisplatin-resistant cells when compared with their cisplatin-sensitive counterparts. *In vitro* cell viability, growth, cell-cycle progression, and apoptosis, as well as *in vivo* therapeutic effectiveness in murine xenograft models, were also assessed following siRNA-mediated c-MYC silencing in cisplatin-resistant ovarian cancer cells. Significant inhibition of cell growth and viability, cell-cycle arrest, and activation of apoptosis were observed upon siRNA-mediated c-MYC depletion. In addition, single weekly doses of c-MYC–siRNA incorporated into 1,2-dioleoyl-sn-glycero-3-phosphocholine (DOPC) 1,2-distearoyl-sn-glycero-3-phosphoethanolamine-N-[methoxy(polyethylene glycol)-2000] (DSPE-PEG-2000)-based nanoliposomes resulted in significant reduction in tumor growth. These findings identify c-MYC as a potential therapeutic target for ovarian cancers expressing high levels of this oncoprotein. *Mol Cancer Ther; 14(10); 2260–9. ©2015 AACR.*

Introduction

The *c-myc* (v-myc avian myelocytomatosis viral oncogene homolog) proto-oncogene belongs to a family of transcription factors characterized by the basic helix–loop–helix leucine-zipper (bHLHZ) motif, which allows binding to specific DNA sequences as multimeric complexes (1, 2). c-MYC regulates the expression of genes involved in a myriad of cellular processes, including replication, growth, metabolism, differentiation, and apoptosis (1–3). Transcriptional activation by c-MYC involves heterodimer complex formation with its protein partner Max (MYC associated factor X), as well as the recruitment of histone acetyltransferases and other coactivators (1, 2, 4–7).

Oncogenic c-MYC arises through multiple molecular mechanisms, including gene amplification, gene translocation, enhanced transcription for other upstream pathways, dysregulation of mRNA-interacting molecules, and decreased rates of ubiquitin-mediated proteolysis (8–10). Overexpression of c-MYC has been reported in most, if not all, types of human malignancies (8, 11, 12). In fact, integrated genome analysis of ovarian carcinoma using The Cancer Genome Atlas (TCGA) project revealed that the most common somatic focal amplification encodes eight genes, including the *c-myc* gene, which is amplified in 30% to 60% of human ovarian tumors (13, 14). In other tumor types, c-MYC expression levels have been associated with drug resistance (15–26).

Current adjuvant chemotherapy for ovarian cancer includes a platinum-based drug such as cisplatin plus a taxane (i.e., paclitaxel; ref. 27). Unfortunately, despite initial response, most patients develop chemoresistant disease, resulting in progressive disease and death (28). Therefore, elucidation of the molecular mechanisms underlying such resistance is imperative to identify novel targets for ovarian cancer therapy. Given the pivotal role of c-MYC in ovarian cancer, its therapeutic targeting in chemoresistance is evident. Here, we examine the biologic and therapeutic effects of targeting c-MYC by siRNAs in cisplatin-resistant cells and in preclinical models of ovarian cancer.

Materials and Methods

Cells and culture conditions

The human ovarian epithelial cancer cells A2780CP20, SKOV3ip1, SKOV3.TR, HEYA8, and HEYA8.MDR were generous gifts from Dr. Anil K. Sood (MD Anderson Cancer Center, Houston, TX), and have been described elsewhere (29, 30). All cell lines were obtained in 2010 and authenticated in 2013 by Promega and ATCC using Short Tandem Repeat (STR) analysis. A2780 and A2780CIS cells were purchased in 2010 from the European

[1]Department of Biochemistry, University of Puerto Rico, Medical Sciences Campus, San Juan, Puerto Rico. [2]Department of Gynecologic Oncology, The University of Texas MD Anderson Cancer Center, Houston, Texas. [3]Center for RNA Interference and Non-Coding RNA, The University of Texas MD Anderson Cancer Center, Houston, Texas. [4]University of Puerto Rico Comprehensive Cancer Center, San Juan, Puerto Rico. [5]Department of Biology, University of Puerto Rico, Rio Piedras Campus, San Juan, Puerto Rico. [6]Department of Cancer Biology, The University of Texas MD Anderson Cancer Center, Houston, Texas.

Note: Supplementary data for this article are available at Molecular Cancer Therapeutics Online (http://mct.aacrjournals.org/).

Corresponding Author: Pablo E. Vivas-Mejía, Comprehensive Cancer Center, University of Puerto Rico, Medical Sciences Campus, San Juan 00935, Puerto Rico. Phone: 787-772-8300; Fax: 787-758-2557; E-mail: pablo.vivas@upr.edu

doi: 10.1158/1535-7163.MCT-14-0801

Collection of Cell Cultures (ECACC), which provides authenticated cell lines. All cell lines (A2780, A2780CP20, A2780CIS, SKOV3ip1, SKOV3.TR, HEYA8, and HEYA8.MDR) were thawed in 2013, expanded, and cryopreserved in several aliquots. Each aliquot was thawed and cultured for no more than 10 to 12 passages. Cells were maintained in RPMI1640 medium supplemented with 10% FBS and 0.1% antibiotic/antimycotic solution in a humidified incubator containing 95% air and 5% CO_2 at 37°C. c-MYC–overexpressing clones and cell clones carrying the empty vectors (EV) were cultured in the same media but containing G418 (500 μg/mL). All tumor cell lines were screened for Mycoplasma using the LookOut Mycoplasma PCR detection kit from Sigma-Aldrich as described by the manufacturer's instructions. *In vitro* assays were performed at 70% to 85% cell density.

Chemicals, reagents, and antibodies

Cisplatin and terbutanol were purchased from Sigma. Cisplatin was reconstituted in 0.9% NaCl. Antibodies against c-MYC, full caspase-3, cleaved caspase-3, full caspase-9, cleaved caspase-9, PARP-1, cyclin D3, cyclin-dependent kinase (CDK) 4, and p27 were purchased from Cell Signaling Technology. β-Actin monoclonal antibody and mouse and rabbit horseradish peroxidase (HRP)-conjugated secondary antibodies were purchased from Sigma. DOPC (1,2-dioleoyl-sn-glycero-3-phosphocholine), DSPE-PEG-2000 (1,2-distearoyl-sn-glycero-3-phosphoethanolamine-N-[methoxy(polyethylene glycol)-2000]), and cholesterol were purchased from Avanti Polar Lipids.

Protein extraction and Western blot analysis

Cells were detached using 0.25% Trypsin-EDTA at 37°C and washed with PBS. Cell lysates were prepared using ice-cold lysis buffer (1% Triton X, 150 mmol/L NaCl, 25 mmol/L Tris HCl, 0.4 mmol/L $NaVO_4$, 0.4 mmol/L NaF, and protease inhibitor cocktail from Sigma), incubated on ice for 30 minutes, and vortex mixed periodically. Lysates were centrifuged, supernatants were collected, and total protein concentration was determined using Bio-Rad DC Protein Assay reagents (Bio-Rad) following the manufacturer's instructions. Equal amounts of each protein sample (typically 30 or 50 μg per lane) were separated by SDS-PAGE, blotted onto nitrocellulose membranes, blocked with 5% non-fat dry milk, rinsed, and probed with the appropriate dilution of the corresponding primary antibody. Following antibody incubation, the membranes were rinsed, incubated with the corresponding HRP-conjugated secondary antibody, and rinsed again. The bound antibodies were detected using enhanced chemiluminescence substrate followed by autoradiography. Bands were imaged and quantified using a FluorChem system (Alpha Innotech Corporation) and AlphaEaseFC software.

siRNAs and *in vitro* siRNA transfection

To silence human c-MYC (NM_002467), two siRNAs targeting exon 2 (5′-GCTTGTACCTGCAGGATCT-3′) and exon 3 (5′-CGTCCAAGCAGAGGAGCAA-3′), and a non-silencing negative control siRNA (C-siRNA) were purchased from Sigma. Briefly, A2780CP20, A2780CIS, and HEYA8 cells (2×10^4 cells/mL or 3.5×10^4 cells/mL) were seeded into 10 cm Petri dishes. Twenty-four hours later, siRNAs were mixed with HiPerFect transfection reagent (Qiagen) at 1:2 (A2780CP20 and A2780CIS) or 1:3 (HEYA8) ratio (siRNA: transfection reagent) in serum and antibiotic-free Opti-MEM medium (Life Technologies). The transfection mix was incubated for 20 minutes at room temperature and then added to the cells. Cells were incubated at 37°C and collected 24 hours after transfection to assess the downregulation of c-MYC by Western blot analysis.

Stable transfections

Ectopic c-MYC expression was performed in cisplatin-sensitive A2780 cells. Briefly, A2780 (4.5×10^4 cells/mL) cells were seeded into 6-well plates. For each well, pcDNA3-cmyc (1.0 μg) (Addgene plasmid 16011, depositor: Wafik El-Deiry) or empty vector (1.0 μg; pcDNA3.1) (Invitrogen, Life Technologies) were mixed with MegaTran 1.0 transfection reagent (1:1 v/v; OriGene) and Opti-MEM medium. The mixture was incubated for 10 minutes at room temperature and added to the cells. Twenty-four hours later, the medium was replaced with fresh RPMI1640 (10% FBS, 0.1% antibiotic/antimycotic solution and 500 μg/mL G418 disulfate salt solution). After 2 to 3 weeks, individual colonies were picked and cultured separately as independent clones.

Cell growth and viability

Cell viability was measured using the Alamar blue dye (Invitrogen) following the manufacturer's instructions. Briefly, A2780CP20 and A2780 cells (2×10^4 cells/mL or 3×10^4 cells/mL) were seeded into 96-well plates. Twenty-four hours later, siRNAs were added to the cells. Seventy-two hours after transfection, the medium was removed and 95 μL of Alamar blue was added. Optical density (OD) values were obtained spectrophotometrically in a plate reader (Bio-Rad) after a maximum of 4 hours of dye incubation. In all cases, percentages of cell viability were obtained after blank OD subtraction, taking the untreated cells values as a normalization control. For combination treatments (siRNAs + cisplatin), OD values were obtained at 96 hours after transfection. For colony formation assays, A2780CP20, A2780CIS, and HEYA8 cells (3×10^4 cells/mL or 4.5×10^4 cells/mL) were seeded into 6-well plates. Twenty-four hours later, siRNAs were added to the cells. Eight hours after transfection, 1,000 (A2780CP20 and HEYA8) or 2,500 (A2780CIS) cells were seeded into 10 cm Petri dishes containing RPMI1640 (10% FBS and 0.1% antibiotic/antimycotic solution) and incubated at 37°C. Seven days (A2780CP20) or 10 days (A2780CIS and HEYA8) later, colony-forming cells were stained with 0.5% crystal violet solution. A2780CP20 and A2780CIS colonies of at least 50 cells were scored under a light microscope (Olympus CKX41) in five random fields with a total magnification of 40×. Visible HEYA8 colonies were counted manually.

Assessment of cell-cycle progression and apoptosis by flow cytometry

To assess cell-cycle progression, A2780CP20 and HEYA8 cells were transfected with siRNAs for 24 hours. Forty-eight hours after transfection, cells were collected, washed in ice-cold PBS, fixed with 70% cold ethanol, and stored at 4°C. Twenty-four hours later, cells were washed with ice-cold PBS, resuspended in propidium iodide (PI)/RNase Staining Buffer (BD Biosciences), incubated in the dark for 15 minutes at room temperature, and then analyzed by flow cytometry in a Beckman Gallios flow cytometer (Beckman Coulter Inc.). FCS Express software (Beckman Coulter) was used to determine the percentage of cells in each phase of the cell cycle. Apoptosis was measured with the fluorescein isothiocyanate (FITC) Annexin V Apoptosis Detection Kit (BD Biosciences), which uses Annexin V and PI as the apoptotic and necrotic markers, respectively. Briefly, A2780CP20 and

HEYA8 cells were transfected with siRNAs for 24 hours. Seventy-two hours after transfection, both floating and attached cells were collected, washed in ice-cold PBS, and resuspended in 1× binding buffer. Cells were then incubated in the dark for 15 minutes at room temperature with Annexin V–FITC and/or propidium iodide according to the manufacturer's instructions. Apoptotic cells were analyzed in a Beckman Gallios flow cytometer. Gallios 1.2 software (Beckman Coulter) was used to determine the percentage of apoptotic and necrotic cells.

siRNA incorporation into DOPC-PEG-nanoliposomes

siRNAs were mixed with DOPC (1:10 w/w), DSPE-PEG-2000 (5% mol/mol of total lipids) and cholesterol (50% w/w of DOPC) in the presence of excess terbutanol (30–35). The mixture was frozen in an acetone-dry ice bath and lyophilized. For *in vivo* administration, the lyophilized powder was hydrated with Ca^{2+} and Mg^{2+}-free PBS at a concentration of 25 mg/mL to achieve the desired dose of 5 μg of siRNA in 200 μL/injection.

Tumor implantation and drug treatment

Female athymic nude mice (NCr-nu, 6 weeks old) were purchased from Taconic. To assess the efficacy of c-MYC silencing *in vivo*, mice were intraperitoneally injected with A2780CP20 cells (1×10^6 cells/0.2 mL HBSS). Three weeks after tumor implantation, mice received two single doses (intraperitoneally) of C-siRNA-DOPC-PEG-nanoliposomes or c-MYC-siRNA-DOPC-PEG-nanoliposomes (5 μg siRNA/injection). Two days after siRNA injection, animals were sacrificed; the peritoneal tumors were harvested and tissue samples were snap-frozen in liquid nitrogen and stored at −80°C for protein analysis by Western blot analysis with a specific antibody against c-MYC. To evaluate the therapeutic activity of c-MYC siRNAs alone or in combination with cisplatin *in vivo*, A2780CP20 cells (1×10^6 cells/0.2 mL HBSS) were injected intraperitoneally. Seven days later, mice were randomly divided into the following treatment groups ($n = 10$/group): (i) C-siRNA, (ii) cisplatin alone, (iii) c-MYC-siRNA, (iv) C-siRNA plus cisplatin, and (v) c-MYC-siRNA plus cisplatin. DOPC-PEG-liposomal-siRNAs (5 μg siRNA/injection) and cisplatin (160 μg/injection) were injected intraperitoneally once a week for 4 weeks. At the end of the treatment, mice were sacrificed and tumors collected. The number of tumor nodules and tumor weight was recorded. The entire peritoneal cavity was examined for tumor metastases.

Characterization of liposomal formulations

Cryo-electron microscopy. The lyophilized liposomal-siRNA powder was resuspended in 500 μL Ca^{2+} and Mg^{2+}-free PBS by ultrasonic agitation for 15 minutes. A 3 μL suspension was applied to fenestrated carbon films blotted to form a vicinal layer, then vitrified in liquid ethane at −180°C. Frozen hydrated samples were observed in a FEI Tecnai TF20 electron microscope (FEI) with a Gatan 626 cryogenic specimen holder (Gatan Inc.), and images recorded on a Falcon2 camera of the same instrument.

Particle size and zeta potential. Light scattering was used to determine the particle size and surface charge (zeta potential) of the liposomal formulations. Liposomes were reconstituted in Ca^{2+} and Mg^{2+}-free PBS and sonicated for 15 to 20 minutes. After sonication, particle size and zeta potential were measured at room temperature with Zeta Pals (Brookhaven Instruments) and Mobius instruments (Wyatt Technology), respectively.

siRNA encapsulation efficiency and siRNA release. Liposomal-siRNAs were reconstituted in Ca^{2+} and Mg^{2+}-free PBS, and sonicated for 15 to 20 minutes. The mixture was added to an Amicon 50K filter (EMD Millipore), and centrifuged at 7,500 rpm for 15 minutes. The eluted fraction was collected to measure the amount of free siRNA using a NanoDrop 2000 spectrophotometer (Thermo Scientific). 0.1% Triton X-100 was then added to the filter, centrifuged again at 7,500 rpm for 15 minutes, and measured spectrophotometrically. This fraction corresponded to the encapsulated siRNA. All experiments included naked-siRNA and empty liposomes (liposomes without siRNA) as controls. The encapsulation efficiency (%E) was calculated using the following equation:

$$\%E = [(\text{total siRNA} - \text{free siRNA})/\text{total siRNA}] \times 100$$

siRNA released from liposomes was calculated by dissolving the liposomal-siRNA in 50% FBS for 0, 2, 8, 24, 48, and 72 hours at 37°C. Liposomes were centrifuged at 7,500 rpm for 15 minutes. Then 0.1% Triton X-100 was added to an Amicon 50K filter and centrifuged again at 7,500 rpm for 15 minutes. The amount of RNA from the Triton X-100 fraction corresponds to the nonreleased siRNA portion. Percentage of release at each time point was calculated using the following equation:

$$\%\text{siRNA released} = [(\text{total siRNA at 0 hours} - \text{siRNA Triton fraction})/\text{total siRNA at 0 hours}] \times 100$$

Biologic half-life (serum stability) and shelf-life. For serum stability, naked-siRNA and liposomal-siRNA were resuspended in 50% FBS and incubated at 37°C. Aliquots were collected at 0, 3, 6, 12, and 24 hours, and frozen at each time point. Prior to electrophoresis, 1% Triton X-100 was added to the aliquots and vortexed-mixed for 2 minutes. 5× loading dye was added and samples were loaded into a 3% agarose gel. Bands were imaged using a FluorChem system (Alpha Innotech) and AlphaEaseFC software. The shelf-life was determined by the conservation of the particle size and surface charge of liposomes at 4°C for 0, 2, and 4 weeks. Similarly, the size and charge of the liposomal formulations were measured at 0, 30, 60, and 120 minutes at room temperature after liposomal reconstitution with Ca^{2+} and Mg^{2+}-free PBS.

In vitro toxicity. *In vitro* toxicity was measured using the Alamar blue dye (Invitrogen) following the manufacturer's instructions. Briefly, A2780CP20 cells (2×10^4 cells/mL) were seeded into 96-well plates. Twenty-four hours later, liposomal formulations (empty liposomes with different DOPC concentrations) were added to the cells. Seventy-two hours after transfection, the medium was removed and 95 μL of Alamar blue was added. OD values were obtained spectrophotometrically in a plate reader (Bio-Rad) after a maximum of 4 hours of dye incubation. In all cases, percentages of cell viability were obtained after blank OD subtraction, taking the untreated cells values as a normalization control.

In vivo safety study (proinflammatory cytokines and blood chemistry). Female wild-type mice (Balb-c, 4 weeks old) were purchased from Taconic. Serum samples were collected from heart blood and further analyzed for proinflammatory cytokine production by ELISA (Qiagen), and blood chemistry [lactate dehydrogenase

(LDH) activity and urea] (Sigma-Aldrich) following the manufacturer's instructions. Briefly, the immune response was evaluated after 5 and 24 hours of intraperitoneal injections (single dose). LDH activity and urea levels were evaluated at 3 weeks (a single injection per day, four consecutive days a week).

Statistical analysis

For *in vitro* and *in vivo* experiments, statistical analysis was performed using Student *t* test for comparing two groups and by ANOVA for multiple group comparisons. *P* values of <0.05 were considered statistically significant. GraphPad Prism software was used for graphing and statistical analysis. Ovarian cancer patient data were downloaded and analyzed from the Cancer Genome Atlas Project (TCGA; http://tcga-data.nci.nih.gov/) for "Ovarian Serous Cystadenocarcinoma" (OV). Level 3 Illumina RNASeq "gene.quantification" files were used to extract MYC expression (RPKM: Reads Per Kilobase of exon model per Million mapped reads) values. Statistical analyses were performed in R (version 3.0.1; http://www.r-project.org/), and the statistical significance was defined as a *P* value of <0.05. The log-rank test was employed to determine the relationship between c-MYC expression and overall/disease-free survival. Kaplan–Meier method was used to generate survival curves. The entire population was randomly split into training (2/3) and validation (1/3) cohorts. In each cohort, patients were divided into percentiles according to c-MYC mRNA expression. Then using the training set, any cut-off between percentiles of 25th and 75th were considered as statistically significant. The statistical significance was corroborated with the validation set.

Results

Expression of c-MYC in human ovarian cancer patients and ovarian cancer cells

To determine potential clinical relevance in drug-resistant ovarian cancer, c-MYC mRNA levels were correlated with clinical data from ovarian cancer patients. Ovarian cancer patient data were downloaded and analyzed from TCGA. Level 3 Illumina RNASeq "gene.quantification" files were used to extract MYC expression. The entire cohort was separated into two sets, the training set (219 patients; Fig. 1A) and the validation set (110 patients; Fig. 1B). The log-rank test revealed that recurrence of disease (expressed as percentage disease free) occurred significantly ($P = 0.0277$) faster for patients with higher c-MYC expression levels (Fig. 1A). These findings were corroborated with further analysis with the validation set ($P = 0.0289$; Fig. 1B). In addition, OS (expressed as the percentage survival) was significantly reduced for patients with higher c-MYC expression values ($P = 0.0058$; Fig. 1C). Statistical analysis with the validation set cohort (Fig. 1D) corroborated these findings ($P = 0.0138$).

To assess c-MYC protein levels, a panel of multiple ovarian cancer cell lines was evaluated by Western blot analysis. Interestingly, cisplatin-resistant cells (A2780CP20 and A2780CIS) expressed higher levels of c-MYC protein when compared with their sensitive counterparts (A2780; Fig. 1E). Densitometric analysis of the band intensities (Fig. 1F) confirmed these findings. The taxane-resistant ovarian cancer cells SKOV3.TR and HEYA8.MDR exhibited similar c-MYC levels when compared with their taxane-sensitive counterparts SKOV3ip1 and HEYA8, respectively. Together, these results suggest that c-MYC is a clinically relevant target for cisplatin-resistant ovarian cancer patients.

Effects of c-MYC silencing on cell growth and viability

Next, we examined the biologic effects of c-MYC silencing in cisplatin-resistant ovarian cancer cells. Western blot analysis confirmed that the two siRNAs used against c-MYC reduced the levels of the c-MYC protein in the A2780CP20 cisplatin-resistant ovarian cancer cell line (Fig. 2A). Densitometric analysis of the band intensities showed that both siRNAs decreased c-MYC expression by more than 80% (****, $P < 0.0001$) compared with C-siRNA (Fig. 2A). Similar results were observed when c-MYC-siRNA was transfected into A2780CIS and HEYA8 ovarian cancer cells (Supplementary Fig. S1A and S1C). Dose-dependent inhibition of cell viability was observed after 72 hours of c-MYC-targeted siRNA treatment (Fig. 2B). The inhibitory effects on viability were observed even at doses as low as 12.5 nmol/L of c-MYC–targeted siRNAs (Fig. 2B). Treatment with c-MYC-siRNA also induced long-term effects in cell growth as evident in colony formation assays (Fig. 2C). Transient transfection of c-MYC-siRNA (2) in A2780CP20 cells significantly reduced (55% reduction; ***, $P < 0.001$) the number of colonies formed after 7 days in culture, compared with the C-siRNA–transfected cells (Fig. 2C). Similarly, transfection of c-MYC–siRNA (2) in A2780CIS and HEYA8 cells significantly reduced (48% and 70% reduction; ****, $P < 0.0001$ and ***, $P < 0.001$, respectively) the number of colonies formed after 10 days in culture (Supplementary Fig. S1B and S1D). On the other hand, silencing c-MYC in A2780 cisplatin-sensitive ovarian cancer cells, which express low c-MYC levels, induced negligible changes in cell viability (Fig. 2D). Combination of a low-active c-MYC-siRNA (2) dose (50 nmol/L, Fig. 2B and 2E) with a relatively low cisplatin dose (2 μmol/L) induced significant (*, $P < 0.05$) additive-like inhibitory effects on the viability of A2780CP20 cells (Fig. 2F) compared with c-MYC-siRNA (2) alone. These data suggest that c-MYC levels are associated with the sensitivity of ovarian cancer cells to cisplatin treatment.

Effects of c-MYC silencing on apoptosis and cell-cycle progression

We next investigated whether the effects induced by c-MYC–siRNA were due to apoptosis, cell-cycle arrest, or both. Transfection of A2780CP20 cells with c-MYC–siRNA (2) induced up to 15% (**, $P < 0.01$) apoptosis compared with cells treated with C-siRNA (Fig. 3A). Western blot analysis showed that siRNA-based c-MYC silencing induced activation of the apoptotic-related molecules caspase-3, caspase-9, and PARP-1 72 hours after transfection (Fig. 3B). Furthermore, 25% of the A2780CP20 cells (****, $P < 0.0001$) were arrested in the G_0–G_1 phase, 48 hours after c-MYC—siRNA (2) transfection (Fig. 3C). Western blot analysis confirmed that key proteins required for transition from G_0–G_1 to S-phase were also altered following c-MYC silencing in A2780CP20 cells (Fig. 3D). Particularly, cyclin D3/cyclin-dependent kinase 4 (CDK4) levels were decreased, while the inhibitory protein of cell-cycle progression, p27, increased in cells treated with c-MYC-siRNA (2) compared with untreated (NT) or C-siRNA–treated cells (Fig. 3D). Densitometric analysis of the band intensities is shown in Fig. 3E. Similar results for apoptosis and cell-cycle progression were observed when c-MYC–siRNA (2) was transfected into HEYA8 ovarian cancer cells (Supplementary Fig. S1E and S1F).

Effect of c-MYC overexpression in the sensitivity of ovarian cancer cells to cisplatin treatment

To confirm the role of c-MYC in the cisplatin resistance of ovarian cancer cells, we performed stable c-MYC transfections in

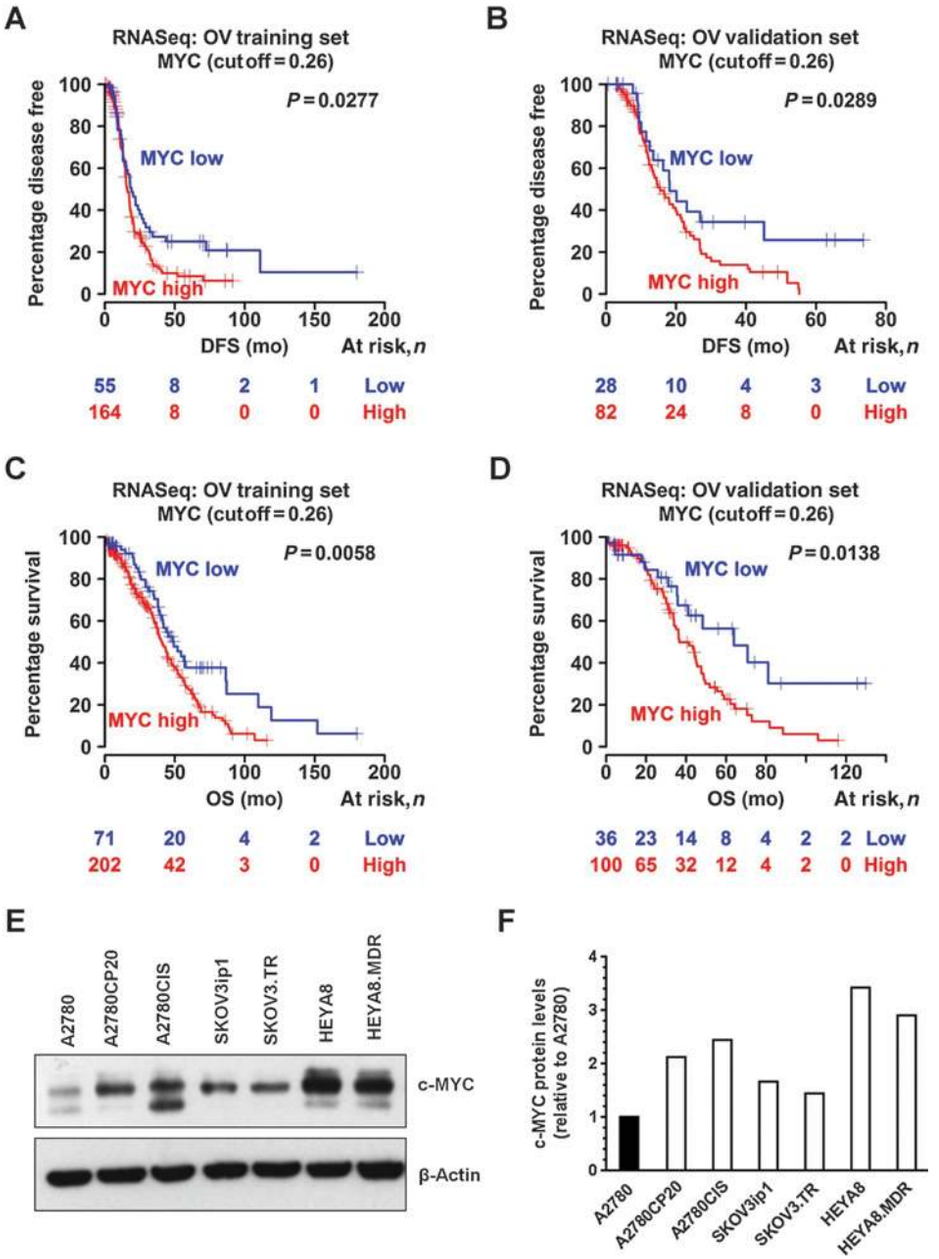

Figure 1.
Expression of c-MYC in ovarian cancer cells and human tumors. Level 3 Illumina RNASeq "gene. quantification" files were used to extract MYC expression. Statistical analysis of c-MYC mRNA expression and clinical data from patients with high-grade serous ovarian cancer showed that the DFS (A and B), and the overall survival (OS; C and D), were significantly reduced for patients with higher c-MYC expression levels. E, Western blot analysis of ovarian cancer cells was performed as described in Materials and Methods. β-Actin was used as a loading control. F, densitometric analysis of the intensities of the bands shown in E. Fold changes in protein levels were calculated relative to A2780 cisplatin-sensitive cells.

A2780 cisplatin-sensitive cells. Figure 4A shows that compared with A2780-untransfected cells (A2780-NT) or with empty vector–transfected clones (A2780-EV), A2780-cmyc clones express higher c-MYC protein levels. At concentrations as low as 1 μmol/L of cisplatin, the c-MYC–overexpressing clones were significantly less sensitive to cisplatin treatment compared with the A2780-untransfected cells or with the EV clones (Fig. 4B). These data suggest that c-MYC contributes to the cisplatin-resistant phenotype observed in ovarian cancer cells.

Characterization of liposomal–siRNA formulations

Particle size and zeta potential of liposomal-siRNA formulations were evaluated by dynamic light scattering, which showed that the liposomes used in this study were slightly negative, and around 100 to 150 nm in diameter (Supplementary Tables S1–S3). The percentage of cholesterol induced changes in the size but not in the surface charge (zeta potential) of the liposomal formulations (Supplementary Table S1). The efficiency of siRNA encapsulation was slightly higher for liposomes with 50% cholesterol (w/w DOPC) as compared with liposomes with 25% cholesterol (w/w DOPC; Supplementary Table S1). The kinetics of siRNA release from liposomes with 25% cholesterol was slower in the first hours compared with liposomes with 50% cholesterol (Supplementary Fig. S2A). However, the kinetics of siRNA release was constant over time for liposomes with 50% cholesterol compared with liposomes with 25%

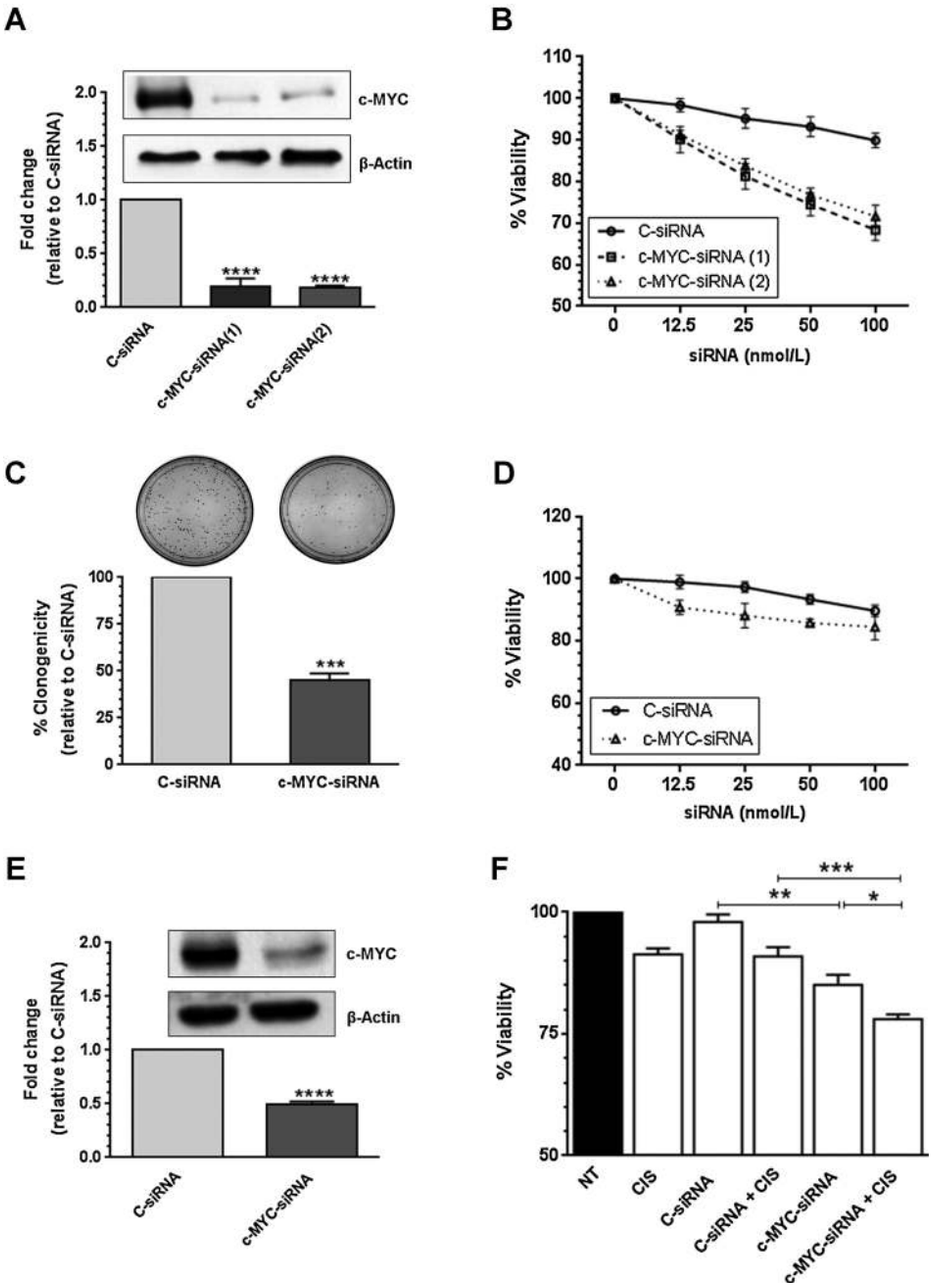

Figure 2.

siRNA-based silencing of c-MYC. Two different siRNAs targeting exon 2 and exon 3 of the human c-MYC sequence (NM_002467) were used. A, A2780CP20 cells (2×10^5) were transfected with 200 nmol/L c-MYC-siRNA. Total protein was isolated from siRNA-transfected cells for Western blot analysis as described in Materials and Methods. Densitometric analysis of the intensities of the bands was calculated relative to the C-siRNA. Averages ± SEM are shown (****, $P < 0.0001$). B, A2780CP20 cells (2×10^3) were seeded into 96-well plates and 24 hours later cells were transfected with a serial dilution of C-siRNA or c-MYC–targeted siRNAs. Cell viability was calculated 72 hours after transfection as described in Materials and Methods. Percentages were obtained after blank OD subtraction, taking the untreated cells values as a normalization control. Averages ± SEM are shown. C, A2780CP20 cells (6×10^4) were seeded into 6-well plates and 24 hours later 100 nmol/L c-MYC-siRNA (2) or 100 nmol/L C-siRNA was added to the cells. Eight hours after transfection, 1,000 cells were seeded into 10-cm Petri dishes. Seven days later, cells were stained and colonies of at least 50 cells were scored under a light microscope. The percentage of clonogenicity was calculated relative to C-siRNA. Averages ± SEM are shown for three independent experiments (***, $P < 0.001$). D, A2780 cells (3×10^3) were seeded into 96-well plates and 24 hours later cells were transfected with a serial dilution of C-siRNA or c-MYC-siRNA (2). Cell viability was calculated as described in B. Averages ± SEM are shown. E, A2780CP20 cells (2×10^5) were transfected with 50 nmol/L c-MYC-siRNA (2). Total protein was isolated from siRNA-transfected cells for Western blot analysis as described in Materials and Methods. Densitometric analysis of the intensities of the bands was calculated relative to the C-siRNA. Averages ± SEM are shown (****, $P < 0.0001$). F, A2780CP20 cells (2×10^3) were seeded into 96-well plates and 24 hours later cells were transfected with 50 nmol/L C-siRNA or 50 nmol/L c-MYC-siRNA (2). The next day, the media was replaced by cisplatin (CIS; 2 μmol/L final concentration) containing RPMI1640 media. Cell viability was calculated 72 hours after CIS treatment (96 hours after transfection) as previously described. Averages ± SEM are shown (*, $P < 0.05$; **, $P < 0.01$; ***, $P < 0.001$).

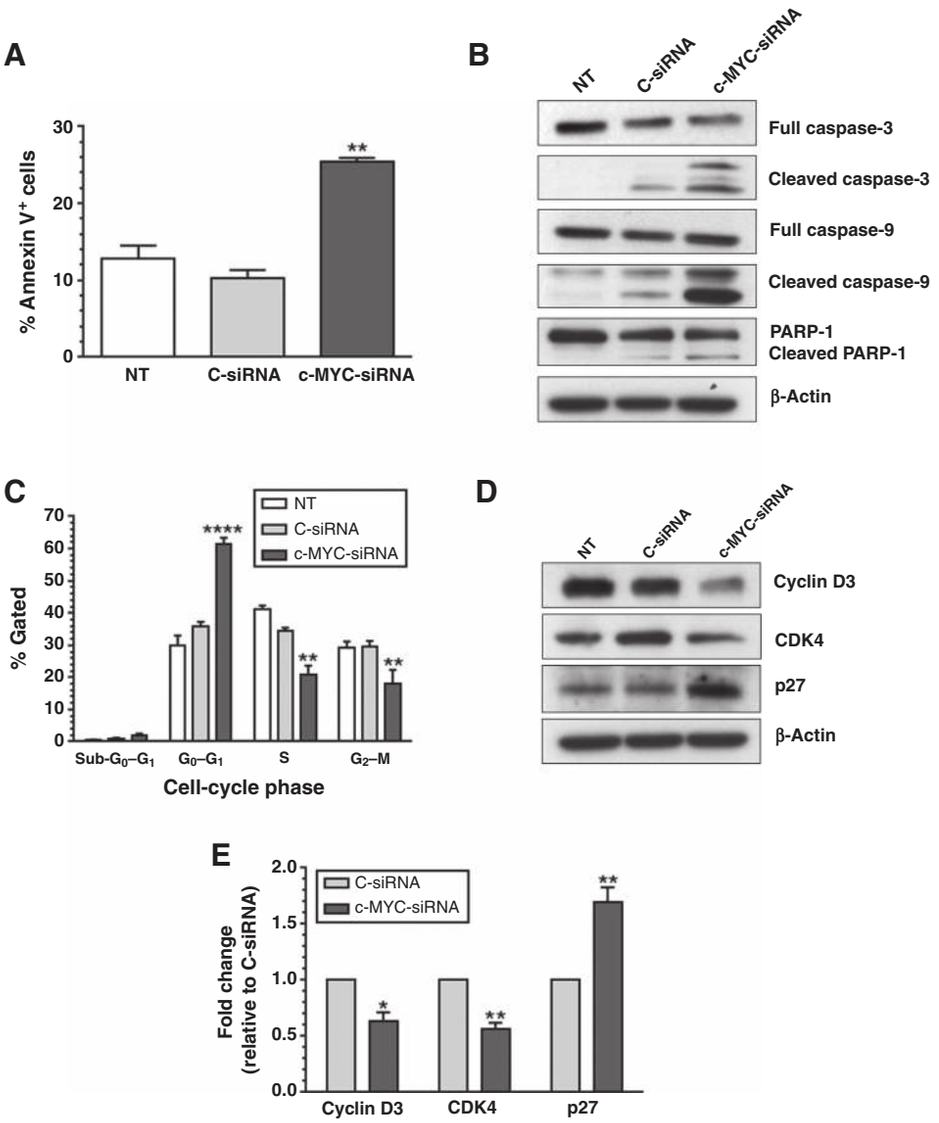

Figure 3.
Apoptosis and cell-cycle progression following c-MYC silencing. Assessment of cell-cycle progression and apoptosis was performed by flow cytometry after siRNA-based c-MYC silencing in cisplatin-resistant cells. A, A2780CP20 cells (6×10^4) were seeded into 6-well plates and 24 hours later 200 nmol/L of C-siRNA or 200 nmol/L of c-MYC-siRNA (2) was added to the cells. Seventy-two hours after transfection, apoptosis was measured with the FITC apoptosis detection kit as described in Materials and Methods. Averages ± SEM are shown for two independent experiments (**, $P < 0.01$). B, A2780CP20 cells (2×10^5) were seeded into 10-cm Petri dishes and transfected as described in A. Western blot analysis was performed 72 hours after transfection for detection of apoptotic-related proteins as described in Materials and Methods. C, A2780CP20 cells (6×10^4) were transfected as described in A. Forty-eight hours after siRNA transfection, A2780CP20 cells were fixed and cell-cycle progression was assessed using PI and the FCS Express software. Averages ± SEM are shown for three independent experiments (**, $P < 0.01$; ****, $P < 0.0001$). D, A2780CP20 cells (2×10^5) were transfected as described in B. Western blot analysis was performed 48 hours after transfection for detection of cell-cycle–related proteins. E, densitometric analysis of the band intensities shown in D are expressed relative to C-siRNA–treated cells. Averages ± SEM are shown for three independent experiments (*, $P < 0.05$; **, $P < 0.01$).

cholesterol. For these reasons, liposomes with 50% cholesterol were used for further studies. A cryo-electron microscopy (cryo-EM) micrograph confirmed the particle size (100–150 nm) and showed that the majority of the liposomes are small unilamellar vesicles (Fig. 4C). The size and charge of the reconstituted liposomal-siRNA formulations were stable over 2 hours at room temperature (Supplementary Table S2) and 4 weeks at 4°C (Supplementary Table S3). The ability of the liposomes to protect the stability of the siRNA from serum nucleases was evaluated *in vitro*. Results showed that siRNA degradation occurred faster for naked-siRNA compared with liposomal-siRNA (Supplementary Fig. S2B). Furthermore, the liposomal-siRNA formulation was not toxic *in vitro* even at DOPC concentrations as high as 50 μmol/L (Supplementary Fig. S2C). *In vivo* studies showed that a single injection of empty liposomes or liposomal-siRNA formulations did not induce early (5 hours) or late (24 hours) immune response (Supplementary Fig. S3A and S3B). Repeated doses of liposomal-siRNA formulations (a single injection per day for 4 days, during 3 weeks) were not toxic for mice as indicated by the LDH activity or urea levels (Supplementary Fig. S3C and S3D), which were similar to the control group (saline solution, only). No weight loss was noted during the treatment period (Supplementary Fig. S3E).

Therapeutic effect of DOPC-PEG-liposomal siRNAs

DOPC-PEG-cholesterol–based nanoliposomes were used for *in vivo* siRNA delivery. First, we assessed whether the c-MYC silencing was effective *in vivo*. Nude mice bearing A2780CP20 tumors were injected intraperitoneally with 2 single doses of 5 μg of DOPC-PEG-liposomal-C-siRNA or 5 μg of DOPC-PEG-liposomal-c-MYC-siRNA. Two days after injection, mice were sacrificed and tumors were dissected. Western blot analysis confirmed that DOPC-PEG-liposomal-c-MYC-siRNA reduced the levels of c-MYC protein at 2 days after injection (Fig. 4D) compared with control groups. Next, the antitumor effects of c-MYC-siRNA as compared with C-siRNA were tested in A2780CP20 tumor-bearing mice. Tumor weight and

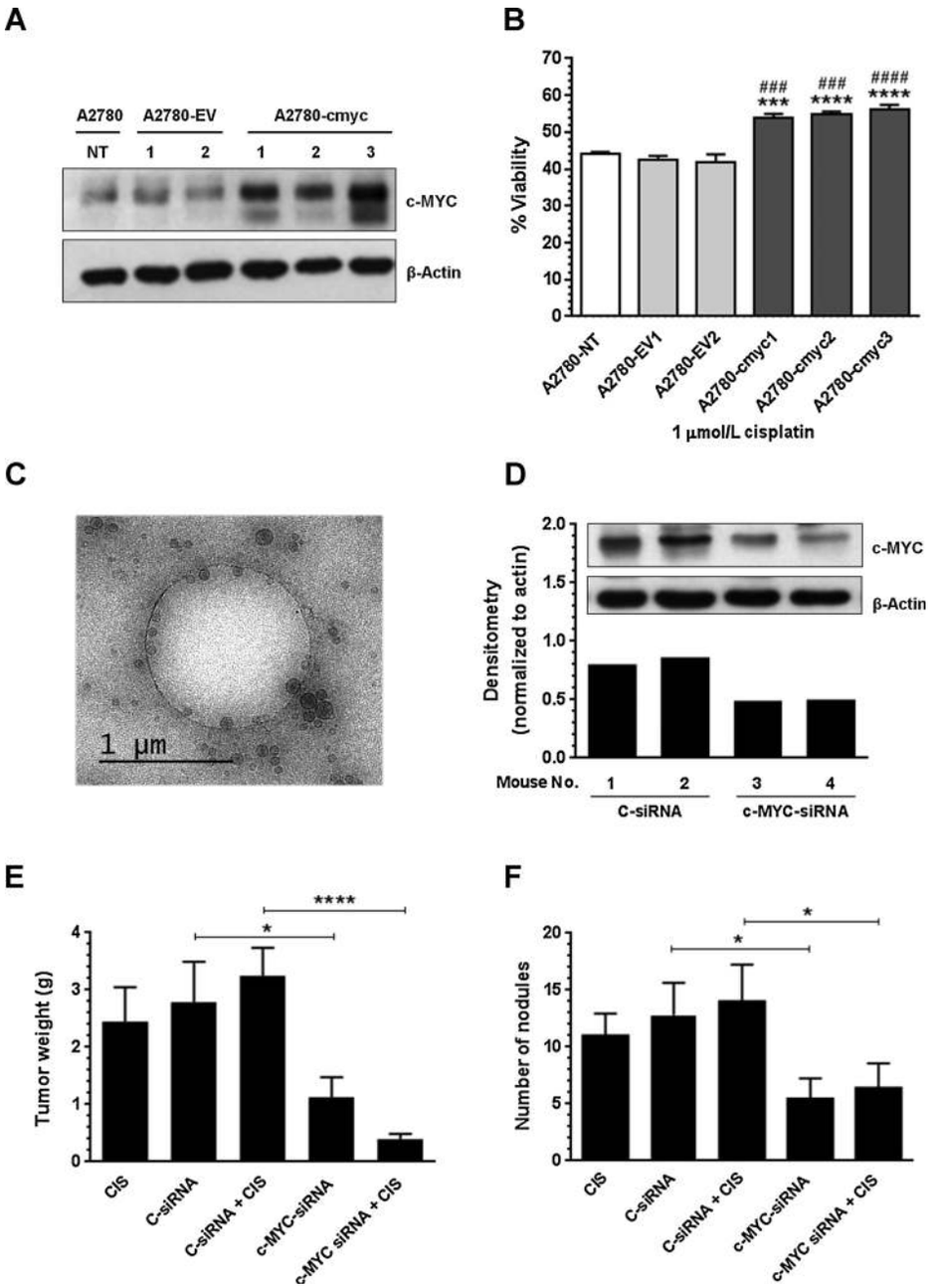

Figure 4.
In vitro effects of c-MYC overexpression and *in vivo* therapeutic efficacy of liposomal c-MYC-siRNA. A2780 cells (9×10^4) were stably transfected with an empty vector (EV) or with a c-MYC–containing vector as described in Materials and Methods. A, Western blot analysis was performed as previously described. Compared with untrasfected cells or with empty vector clones, the c-MYC–overexpressing clones showed higher c-MYC protein levels. B, stable transfected A2780 cells were exposed to CIS (1 μmol/L final concentration) containing RPMI1640 media. Cell viability was calculated as described in Materials and Methods. Averages ± SEM are shown relative to A2780-EV1 (***, $P < 0.001$; ****, $P < 0.0001$) or to A2780-EV2 (###, $P < 0.001$; ####, $P < 0.0001$). Lyophilized liposomal-siRNAs were reconstituted in Ca^{2+} and Mg^{2+}-free PBS. C, cryo-EM shows that the majority of the particles are small unilamellar vesicles in the 100 to 150 nm range. The hole in the image is a fenestration in the carbon support, which measures 1.2 μm in diameter. Nude mice were injected intraperitoneally with A2780CP20 cells and randomly allocated in the groups described in Materials and Methods. D, Western blot analysis shows that c-MYC-siRNA-DOPC-PEG treatment reduced c-MYC protein levels *in vivo*. Therapy began 1 week after tumor cell inoculation. E, mean tumor weight and number of nodules was recorded after 4 weeks (F). Averages ± SEM are shown (*, $P < 0.05$; ****, $P < 0.0001$).

number of nodules were assessed in five treatment groups (10 mice each): (i) C-siRNA, (ii) cisplatin alone, (iii) c-MYC-siRNA, (iv) C-siRNA plus cisplatin, and (v) c-MYC-siRNA plus cisplatin. All DOPC-PEG-liposomal siRNAs (5 μg siRNA/injection) and cisplatin (160 μg/injection) treatments were injected intraperitoneally once per week for 4 weeks. No weight loss was noted during the treatment period (Supplementary Fig. S3F). Cisplatin treatment by itself did not induce a significant effect on tumor growth (Fig. 4E). On the other hand, decreased tumor weight was observed in the c-MYC-siRNA group (*, $P < 0.05$) compared with the C-siRNA group (Fig. 4E). In addition, c-MYC-siRNA induced a decrease in the number of tumor nodules (*, $P < 0.05$) compared with the C-siRNA group (Fig. 4F).

Discussion

In this study, we showed that high levels of c-MYC are associated with faster recurrence and poor overall survival of patients with high-grade serous ovarian cancer, and with cisplatin resistance in ovarian cancer cells. Another key finding was that siRNA-based silencing of c-MYC inhibits cell growth *in vitro* and reduces tumor growth in xenograft models of cisplatin-resistant ovarian

cancer. c-MYC, an oncoprotein highly abundant in several types of cancer, is considered an undruggable molecule by virtue of its flat protein surface (36, 37). Thus, the evidence we present here suggests that siRNA-based c-MYC targeting is a therapeutic modality for ovarian cancer patients expressing high c-MYC levels, including those that are resistant to cisplatin treatment.

The c-MYC transcription factor, which regulates 15% of all human genes, plays an important role in a myriad of biologic processes, including cell growth and proliferation, cell-cycle progression, apoptosis, angiogenesis, senescence, and genomic instability (1–3, 38, 39). In addition, c-MYC regulates the expression of not only a particular group of genes but acts in concert with RNA polymerase and transcription factors as a universal amplifier of gene expression in embryonic stem cells (40) and tumor cells (41). In fact, *c-myc* amplification has been reported in multiple malignancies, including ovarian cancer (14). In other tumor types, c-MYC expression levels have been associated with drug resistance (15–26). For instance, Sakamuro and colleagues have shown that c-MYC oncoprotein increases cisplatin resistance by decreasing production of the c-MYC inhibitor bridging integrator 1 (BIN1; ref. 16). Our findings related to the role of ectopic expression of c-MYC in decreasing the sensitivity of ovarian cancer cells to cisplatin treatment are in agreement with these reports.

The therapeutic effects of siRNA-based c-MYC silencing in cisplatin-resistant ovarian cancer cells have not been fully addressed. Current adjuvant chemotherapy for ovarian cancer includes cisplatin and paclitaxel; unfortunately, the majority of the patients develop chemoresistance that leads to therapeutic failure (27, 28). Thus, our study provides further evidence that c-MYC is a plausible target for ovarian cancer patients with high c-MYC expression levels. Moreover, the findings that the c-MYC–targeted siRNA did not affect the viability of cells with low c-MYC protein levels, suggests that c-MYC could be considered as a potential biomarker and an indicative of chemotherapy response. Nevertheless, the results that siRNA-mediated c-MYC silencing induced more pronounced effects in c-MYC downregulation than in cell growth and viability confirm previous findings (42) that molecular pathways other than c-MYC upregulation contribute to the cisplatin resistance of ovarian cancer cells. These results suggest that therapies targeting different cell survival pathways should be more beneficial than targeting a single pathway in advanced and drug-resistant ovarian cancer.

We have shown that c-MYC siRNA–based silencing induces short- and long-term effects in cell growth and viability. These effects were associated with both apoptosis induction and cell-cycle arrest. Future studies should determine the c-MYC–regulated antiapoptotic genes associated with the cisplatin resistance in ovarian cancer cells. In agreement with previous studies (14, 43), one of the major cell-cycle–inhibitory proteins, p27, was increased following c-MYC depletion. Similarly, decreased levels of CDK4 and cyclin D3 following c-MYC silencing probably occurred by the ability of c-MYC to transcriptionally regulate the expression of these proteins (44).

In conclusion, we present evidence here that DOPC-PEG-liposomal c-MYC–targeted siRNA alone or in combination with chemotherapy is efficacious in preclinical models. Further pharmacodynamic, pharmacokinetic, and tissue distribution studies will be required prior to clinical translation.

Disclosure of Potential Conflicts of Interest

No potential conflicts of interest were disclosed.

Authors' Contributions

Conception and design: J.M. Reyes-González, A.K. Sood, P.E. Vivas-Mejia
Development of methodology: J.M. Reyes-González, G.N. Armaiz-Peña, I.M. Echevarría-Vargas, A. Rivera-Reyes, P.E. Vivas-Mejía
Acquisition of data (provided animals, acquired and managed patients, provided facilities, etc.): J.M. Reyes-González, G.N. Armaiz-Peña, F. Valiyeva, S. Pradeep, P.E. Vivas-Mejía
Analysis and interpretation of data (e.g., statistical analysis, biostatistics, computational analysis): J.M. Reyes-González, G.N. Armaiz-Peña, L.S. Mangala, C. Ivan, A.K. Sood, P.E. Vivas-Mejía
Writing, review, and/or revision of the manuscript: J.M. Reyes-González, A.K. Sood, P.E. Vivas-Mejía
Administrative, technical, or material support (i.e., reporting or organizing data, constructing databases): A.K. Sood
Study supervision: L.S. Mangala, A.K. Sood, P.E. Vivas-Mejía

Grant Support

This project was supported partially by the NIH/NCI 1K22CA166226-01A1 and institutional seed funds from the University of Puerto Rico Comprehensive Cancer Center (to P.E. Vivas-Mejía); and the NIH, Minority Biomedical Research Support (MBRS) RISE Grant Number R25GM061838 (to J.M. Reyes-González). This project was also supported partially by CA016672, P50 CA083639, U54 CA151668, UH2 TR000943, the Blanton-Davis Ovarian Cancer Research Program, the RGK Foundation, the Gilder Foundation, and the Betty Anne Asche Murray Distinguished Professorship (to A.K. Sood).

The costs of publication of this article were defrayed in part by the payment of page charges. This article must therefore be hereby marked *advertisement* in accordance with 18 U.S.C. Section 1734 solely to indicate this fact.

Received September 18, 2014; revised July 1, 2015; accepted July 19, 2015; published OnlineFirst July 30, 2015.

References

1. Eilers M, Eisenman RN. Myc's broad reach. Genes Dev 2008;22:2755–66.
2. Grandori C, Cowley SM, James LP, Eisenman RN. The Myc/Max/Mad network and the transcriptional control of cell behavior. Annu Rev Cell Dev Biol 2000;16:653–99.
3. Bui T V, Mendell JT. Myc: Maestro of microRNAs. Genes Cancer 2010;1:568–75.
4. Knoepfler PS. Myc goes global: new tricks for an old oncogene. Cancer Res 2007;67:5061–3.
5. McMahon SB, Wood MA, Cole MD. The essential cofactor TRRAP recruits the histone acetyltransferase hGCN5 to c-Myc. Mol Cell Biol 2000;20:556–62.
6. McMahon SB, Van Buskirk HA, Dugan KA, Copeland TD, Cole MD. The novel ATM-related protein TRRAP is an essential cofactor for the c-Myc and E2F oncoproteins. Cell 1998;94:363–74.
7. Frank SR, Parisi T, Taubert S, Fernandez P, Fuchs M, Chan H-M, et al. MYC recruits the TIP60 histone acetyltransferase complex to chromatin. EMBO Rep 2003;4:575–80.
8. Vita M, Henriksson M. The Myc oncoprotein as a therapeutic target for human cancer. Semin Cancer Biol 2006;16:318–30.
9. Dang C V. MYC on the path to cancer. Cell 2012;149:22–35.
10. Choi SH, Wright JB, Gerber SA, Cole MD. Myc protein is stabilized by suppression of a novel E3 ligase complex in cancer cells. Genes Dev 2010;24:1236–41.
11. Eisenman RN. Deconstructing myc. Genes Dev 2001;15:2023–30.
12. Baker V V, Borst MP, Dixon D, Hatch KD, Shingleton HM, Miller D. c-myc amplification in ovarian cancer. Gynecol Oncol 1990;38:340–2.
13. Cancer Genome Atlas Research Network. Integrated genomic analyses of ovarian carcinoma. Nature 2011;474:609–15.

14. Prathapam T, Aleshin A, Guan Y, Gray JW, Martin GS. p27Kip1 mediates addiction of ovarian cancer cells to MYCC (c-MYC) and their dependence on MYC paralogs. J Biol Chem 2010;285:32529–38.
15. Torigoe T, Izumi H, Ishiguchi H, Yoshida Y, Tanabe M, Yoshida T, et al. Cisplatin resistance and transcription factors. Curr Med Chem Anticancer Agents 2005;5:15–27.
16. Pyndiah S, Tanida S, Ahmed KM, Cassimere EK, Choe C, Sakamuro D. c-MYC suppresses BIN1 to release poly(ADP-ribose) polymerase 1: a mechanism by which cancer cells acquire cisplatin resistance. Sci Signal 2011;4: ra19.
17. Lin C-P, Liu J-D, Chow J-M, Liu C-R, Liu HE. Small-molecule c-Myc inhibitor, 10058-F4, inhibits proliferation, downregulates human telomerase reverse transcriptase and enhances chemosensitivity in human hepatocellular carcinoma cells. Anticancer Drugs 2007;18:161–70.
18. Leonetti C, Biroccio A, Benassi B, Stringaro A, Stoppacciaro A, Semple SC, et al. Encapsulation of c-myc antisense oligodeoxynucleotides in lipid particles improves antitumoral efficacy in vivo in a human melanoma line. Cancer Gene Ther 2001;8:459–68.
19. Biroccio A, Benassi B, Amodei S, Gabellini C, Del Bufalo D, Zupi G. c-Myc down-regulation increases susceptibility to cisplatin through reactive oxygen species-mediated apoptosis in M14 human melanoma cells. Mol Pharmacol 2001;60:174–82.
20. Sklar MD, Prochownik E V. Modulation of cis-platinum resistance in Friend erythroleukemia cells by c-myc. Cancer Res 1991;51:2118–23.
21. Leonetti C, Biroccio A, Candiloro A, Citro G, Fornari C, Mottolese M, et al. Increase of cisplatin sensitivity by c-myc antisense oligodeoxynucleotides in a human metastatic melanoma inherently resistant to cisplatin. Clin Cancer Res 1999;5:2588–95.
22. Citro G, D'Agnano I, Leonetti C, Perini R, Bucci B, Zon G, et al. c-myc antisense oligodeoxynucleotides enhance the efficacy of cisplatin in melanoma chemotherapy in vitro and in nude mice. Cancer Res 1998;58:283–9.
23. Xie X-K, Yang D-S, Ye Z-M, Tao H-M. Recombinant antisense C-myc adenovirus increase in vitro sensitivity of osteosarcoma MG-63 cells to cisplatin. Cancer Invest 2006;24:1–8.
24. Knapp DC, Mata JE, Reddy MT, Devi GR, Iversen PL. Resistance to chemotherapeutic drugs overcome by c-Myc inhibition in a Lewis lung carcinoma murine model. Anticancer Drugs 2003;14:39–47.
25. Walker TL, White JD, Esdale WJ, Burton MA, DeCruz EE. Tumour cells surviving in vivo cisplatin chemotherapy display elevated c-myc expression. Br J Cancer 1996;73:610–4.
26. Mizutani Y, Fukumoto M, Bonavida B, Yoshida O. Enhancement of sensitivity of urinary bladder tumor cells to cisplatin by c-myc antisense oligonucleotide. Cancer 1994;74:2546–54.
27. Gamarra-Luques CD, Goyeneche AA, Hapon MB, Telleria CM. Mifepristone prevents repopulation of ovarian cancer cells escaping cisplatin-paclitaxel therapy. BMC Cancer 2012;12:200.
28. Herzog TJ. Recurrent ovarian cancer: how important is it to treat to disease progression? Clin Cancer Res 2004;10:7439–49.
29. Vivas-Mejia PE, Rodriguez-Aguayo C, Han H-D, Shahzad MMK, Valiyeva F, Shibayama M, et al. Silencing survivin splice variant 2B leads to antitumor activity in taxane–resistant ovarian cancer. Clin Cancer Res 2011;17: 3716–26.
30. Vivas-Mejia P, Benito JM, Fernandez A, Han H-D, Mangala L, Rodriguez-Aguayo C, et al. c-Jun-NH2-kinase-1 inhibition leads to antitumor activity in ovarian cancer. Clin Cancer Res 2010;16:184–94.
31. Tanaka T, Mangala LS, Vivas-Mejia PE, Nieves-Alicea R, Mann AP, Mora E, et al. Sustained small interfering RNA delivery by mesoporous silicon particles. Cancer Res 2010;70:3687–96.
32. Shaw TJ, Senterman MK, Dawson K, Crane CA, Vanderhyden BC. Characterization of intraperitoneal, orthotopic, and metastatic xenograft models of human ovarian cancer. Mol Ther 2004;10:1032–42.
33. Landen CN, Goodman B, Katre AA, Steg AD, Nick AM, Stone RL, et al. Targeting aldehyde dehydrogenase cancer stem cells in ovarian cancer. Mol Cancer Ther 2010;9:3186–99.
34. Landen CN, Chavez-Reyes A, Bucana C, Schmandt R, Deavers MT, Lopez-Berestein G, et al. Therapeutic EphA2 gene targeting in vivo using neutral liposomal small interfering RNA delivery. Cancer Res 2005;65:6910–8.
35. Landen CN, Merritt WM, Mangala LS, Sanguino AM, Bucana C, Lu C, et al. Intraperitoneal delivery of liposomal siRNA for therapy of advanced ovarian cancer. Cancer Biol Ther 2006;5:1708–13.
36. Verdine GL, Walensky LD. The challenge of drugging undruggable targets in cancer: lessons learned from targeting BCL-2 family members. Clin Cancer Res 2007;13:7264–70.
37. Horiuchi D, Anderton B, Goga A. Taking on Challenging Targets: Making MYC Druggable. Am Soc Clin Oncol Educ Book 2014;34:e497–502.
38. Vervoorts J, Lüscher-Firzlaff J, Lüscher B. The ins and outs of MYC regulation by posttranslational mechanisms. J Biol Chem 2006;281: 34725–9.
39. Frenzel A, Lovén J, Henriksson MA. Targeting MYC-Regulated miRNAs to Combat Cancer. Genes Cancer 2010;1:660–7.
40. Nie Z, Hu G, Wei G, Cui K, Yamane A, Resch W, et al. c-Myc is a universal amplifier of expressed genes in lymphocytes and embryonic stem cells. Cell 2012;151:68–79.
41. Lin CY, Lovén J, Rahl PB, Paranal RM, Burge CB, Bradner JE, et al. Transcriptional amplification in tumor cells with elevated c-Myc. Cell 2012;151:56–67.
42. Echevarría-Vargas IM, Valiyeva F, Vivas-Mejía PE. Upregulation of miR-21 in cisplatin resistant ovarian cancer via JNK-1/c-Jun pathway. PLoS ONE 2014;9:e97094.
43. D'Agnano I, Valentini A, Fornari C, Bucci B, Starace G, Felsani A, et al. Myc down-regulation induces apoptosis in M14 melanoma cells by increasing p27(kip1) levels. Oncogene 2001;20:2814–25.
44. Qi Y, Tu Y, Yang D, Chen Q, Xiao J, Chen Y, et al. Cyclin A but not cyclin D1 is essential for c-myc-modulated cell-cycle progression. J Cell Physiol 2007;210:63–71.